Materials Science and Engineering C 71 (2017) 735–743

Contents lists available at ScienceDirect

Materials Science and Engineering C

journal homepage: www.elsevier.com/locate/msec

Sustained drug release and electrochemical performance of ethyl cellulose-magnesium hydrogen phosphate composite

Faruq Mohammad [a,*], Tanvir Arfin [b,*], Hamad A. Al-Lohedan [a]

[a] Surfactant Research chair, Department of Chemistry, College of Science, King Saud University, P.O. Box 2455, Riyadh 11451, Saudi Arabia
[b] Environmental Materials Division, CSIR-National Environmental Engineering Research Institute (CSIR-NEERI), Nehru Marg, Nagpur 440020, India

ARTICLE INFO

Article history:
Received 20 July 2016
Received in revised form 28 September 2016
Accepted 24 October 2016
Available online 26 October 2016

Keywords:
Organic-inorganic composites
Ethyl cellulose
$MgHPO_4$
Conductivity
Drug delivery
Proguanil drug

ABSTRACT

In this, a sol-gel method was applied to prepare ethyl cellulose-magnesium hydrogen phosphate (EC-$MgHPO_4$) composite that can have potential applications in the sensory, pharmaceutical, and biomedical sectors. The formed composite was thoroughly characterized by making use of the instrumental analysis such as UV–Vis, FT-IR, HRTEM, EDAX, SEM and XRD. For the composite, the other parameters determined includes the water uptake, porosity, thickness, bulk and tapped densities, angle of repose, Carr's index and Hausner ratio. From the results, the material found to exhibit good flowing properties with a Carr's index of 11.11%, Hausner ratio of 1.125, and angle of response of 33°. The EDAX spectrum and HRTEM analysis confirmed for the composite formation and the particles size is investigated to be around 52 nm. The surface porosity due to the EC matrices was confirmed by the SEM analysis, which further used for the loading of drug, Proguanil. In addition, the material's conductivity was studied by taking uni-univalent electrolyte solution (KCl and NaCl) indicated that the conductivity follows the order of KCl > NaCl, while the activation energy obtained from Arrhenius method resembled that the conductivity is strongly influenced by the electrolyte type used. We found from the analysis that, with a decrease in the size of hydrated radii of ions, the conductivity of EC-$MgHPO_4$ material also observed to be decreased in the order $K^+ > Na^+$ and the material proved to be mechanically stable and can be operated over a range of pHs, temperatures, and electrolyte solutions. Further, the drug loading and efficiency studies indicated that the material can trap up to 80% of Proguanil (antimalarial drug) applied for its loading. The Proguanil drug release profiles confirmed for the controlled and sustained release from the EC-$MgHPO_4$ matrix, as the material can release up to 87% of its total loaded drug over a 90 min period. Finally, the cell viability and proliferation studies tested against two different cell cultures of BRL-3A rat liver and H9c2 cardiomyoblasts indicated the non-toxic nature and safer applicability of the EC-$MgHPO_4$ (25–500 μg/mL, 24 h). Overall, the results of the study confirm for the safer applicability of the composite towards biosensor, drug delivery, scaffolding, and bioanalytical (quality control) applications.

1. Introduction

In the present scientific research, the organic-inorganic hybrid materials have gained much attention of researchers due to their outstanding mechanical properties combined with some other integrated characteristics such as thermally stable inorganic backbones, specific chemical reactivity and flexibility inorganic functional groups, in addition to non-toxic nature [1–5]. Thus formed hybrid material's inclined properties are highly dependent on their chemical composition, dynamic structure, porosity and other surface characteristics. The water dispersibility, solubility and mechanical toughness are some of the potential advantages offered by the hybrid composites. Also, in order to manufacture these composites, the sol-gel mediated formation of hybrid matrices was considered as the active means because of the creation of complex structures with high stabilities, minimum swelling properties, controlled cross-linking, and effective bond formation between the organic and inorganic segments [6–8].

One of the derivatives of cellulose, ethyl cellulose (EC) exhibits the properties of extensive linearity, chain stiffness, good solubility in organic solvents, good biocompatibility, high mechanical intensity, and stability which can be explored for the formation of hybrid composites in combination with various other materials [9]. It is considered to be one of the exclusive derivatives of cellulose obtained from inexhaustible natural polymers and is formed by the

Abbreviations: EC, ethyl cellulose; $MgHPO_4$, magnesium hydrogen phosphate; CBPC, chemically bonded phosphate ceramics; XRD, x-ray diffraction; EDAX, electron diffraction analysis by x-rays; FT-IR, fourier transform-infrared; HRTEM, high resolution transmission electron microscopy; SEM, scanning electron microscopy.

* Corresponding authors.
E-mail addresses: fmohammad@ksu.edu.sa (F. Mohammad), t_arfin@neeri.res.in (T. Arfin).

http://dx.doi.org/10.1016/j.msec.2016.10.062
0928-4931/

conversion of the hydroxyl groups on the repeated glucose units into ethyl ether groups. The different applications of EC are in paper and textile coatings, gel lacquers, food additives as an emulsifier and on large extent, it is employed as a dissolution rate controlling polymer in sustained release dosage forms [10–11]. In addition, the physicochemical properties like compressibility, passive, and hydrophobic behavior especially attracted for its use in the preparation of lipophilic pharmaceutical dosage forms by taking advantage of its nontoxic, stable, ease of processing and low cost nature combined in a biodegradable form [12].

In recent years, the interesting properties of phosphate materials such as high thermal expansion coefficient, low glass transition temperature and low softening temperature have attracted attention of researchers [13]. Since, these materials are considered to be potentially eligible for making solid state electrolytes, machinable glass ceramics, amorphous semiconductors, laser glasses, optoelectronic and nuclear waste storage materials [14–16]. Among many other phosphates, the spectroscopic appearance of the vibration modes in the magnesium phosphate ($MgHPO_4$) compound is very complex at least due to the coupling effects and also due to the presence of Mg^{2+}, $H_2PO_4^-$ and H_2O species [17]. The magnesium phosphate cement, also called magnesium phosphate ceramics, falls into the category of chemically bonded phosphate ceramics (CBPC) and is highly crystalline in nature and is regarded as the room temperature-setting ceramics analyzed for the use of structural materials [18].

The analytical chemistry, process industry, food analysis and water-quality control are the various fields where the electrolyte conductivity measurements are highly applicable [19]. In addition, the medical fields like pharmacology, blood and urea analysis, tissue-perfusion measurements, chemical and biological sensing for the detection of a wide range of biochemical species such as amino acids, proteins, peptides, DNA, explosives and chemical warfare agents also takes the tools of conductivity measurements [20]. Further in pharmaceutical industry, it is highly important to report the powder flow properties of the crystalline/amorphous materials and for that, the physical parameters in general are measured by taking the thickness, water uptake, porosity, bulk density, tapped density, angle of response, Carr's index, and Hausner ratio. The bulk density of a powdered composite is denoted by the weight in a given volume (including interparticulate void volume), while the tapped density measures the density after mechanically tapping the container having the powder sample. The Carr's index is an indicative of powder bridge strength and stability, while the Hausner ratio represents interparticle friction.

With that, the objective of the present study was to prepare an inorganic-organic hybrid composite material which has the broader range of applications in the pharmaceutical and biomedical sector by taking advantage of its controllable properties of conductivity, biodegradability and surface adsorption. For that, we prepared a stable EC-$MgHPO_4$ composite using sol-gel approach involving EC as binder and $MgHPO_4$ of semiconductor material in a 1:3 wt/wt. ratio. We hypothesized that the formed hybrid composite of EC-$MgHPO_4$ be suitable for the integrated applications by taking advantage of its biodegradable and adsorption properties provided by EC (suitable for the controlled drug delivery applications), and electrochemical conductivity due to $MgHPO_4$ (offers biosensing capacity). The other applications of the formed composite can be in the filtration tasks in the beverage and textile industry, medicine, chemical industry, and waste-water treatment. All the above mentioned applications are ascribed to their high thermal and chemical resistances, mechanical strength, simplicity and low operation costs. In the study, the formed EC-$MgHPO_4$ composite was thoroughly characterized by using the instrumental analysis such as UV–Vis, FT-IR, HRTEM, SEM, EDAX, and powdered XRD measurements. Further, the composite was loaded with Proguanil, an *anti*-malarial drug to see its controlled biodegradable properties by means of investigating the release of the drug from the surface of EC due to the variations in pH, and temperature. Also, the conductivity behavior was investigated by measuring the electrochemical behavior under the influence of different solution mediums. Finally, the composite was tested for its toxicity following the treatment to two different cell cultures of BRL-3A rat liver cells and H9c2 cardiomyoblsts over a range of concentrations of 25–500 μg/mL for a 24 h period.

2. Experimental

2.1. Synthesis of EC-$MgHPO_4$ composite

The synthesis method for the preparation of EC-$MgHPO_4$ was similar to as followed by Arfin and Kumar [21]. Briefly, 0.2 M dipotassium hydrogen orthophosphate (98%, S.D. Fine-Chem Limited) was mixed with 0.2 M magnesium(II) chloride (99%, S.D. Fine-Chem Limited) to yield light white precipitate. To this mixture, dilute hydrochloric acid (35.4%, S.D. Fine-Chem Limited) was added so as to maintain the pH at 1.0 by stirring constantly for some time whereas the precipitate was kept at room temperature (24 h) for the observation. For the removal of free electrolytes, the precipitate was well washed with deionized water and was dried at 50 °C. By using a mortar and pestle, the dried precipitate was churned into powder and then sieved by using 85 μm sieve. The expected chemical equation is as given below:

$$MgCl_2 + K_2HPO_4 \rightarrow MgHPO_4 + 2KCl$$

To this, pure ethyl cellulose, EC (99%, S.D. Fine-Chem Limited) was employed as binder, grounded and sieved through 85 μm mesh. Different combinations of the ratio of precipitate and binder were analyzed so as to obtain the final composite material consisting of efficient mechanical strength and electrical conductivity. In that view, we found that the material prepared by embedding 25% EC was considered to be highly applicable for the experimentation. However, the material with high EC content was found to be stable but the electrical conductivity is becoming a major issue, while the composite of lesser amount of EC suffers from the issues related to mechanical instability. For the preparation of composite with 25% EC, we first placed 63 mg of EC and 187 mg of $MgHPO_4$ in an oven at 80 °C for about 30 min, and further increased the temperature to around 90 °C for 15 mins so as to equilibrate the reactants mixture. After cooling of the contents to room temperature, the tablets are formed by compressing the composite mixture using a Tablet compression (Mini press 1 station, Rimek). The tablets formed from the powder composite are shown in Fig. 1.

2.2. Measurement of material conductivity

The construction of concentration cells were organized to measure the material conductivity for evaluating the activation energy. For the

Fig. 1. Formation of tablets from the powdered composite of EC-$MgHPO_4$.

electrochemical measurements, the test cell utilized was same as that described elsewhere [22]. For the measurements, the prepared materials were inserted as if it was sandwiched between the two glass half-cells which had a hole to introduce the electrolyte solution where the half-cell volume was 20 mL and the effective material area was 60.13 mm^2. The KCl and NaCl solutions of varied concentrations were prepared by utilizing the deionized water. For minimizing the concentration-polarization at the material surfaces, a magnetic stirrer was kept at the bottom of each half-cell where the estimation of the solutions was done at a stirring rate. The pH of solutions was noted in the range of 5.5 to 6. Different effective and qualitative methods were assumed for measuring the conductivity [23] at different temperatures (5 ± 50) ± 0.2 °C. By employing an auto ranging digital conductivity meter such as Model no. EQ-667 Equip-Tronics, the material conductivity was measured. For the accuracy of results, three individual measurements of the conductivity were taken into account and the mean of it was considered as final.

2.3. Proguanil drug loading and release studies

For the loading of Proguanil (95%, Sigma-Aldrich) *anti*-malarial drug onto the EC-$MgHPO_4$ composite, we followed the simple adsorption method, but not the chemical bonding technique where it is prone to affect the therapeutic efficacy of the drug. For the adsorption of drug, an aqueous solution containing Proguanil hydrochloride (at a concentration of 0.5 mg/mL) was added dropwise to a colloidal suspension of EC-$MgHPO_4$ composite in distilled water (of 0.5 mg/mL concentration) under sonication. The sonication was continued for 4 h, and following the period, the precipitate was separated out from the supernatant by means of centrifugation, washed the precipitate with distilled water 2–3 times and dried at room temperature to get the powder. By taking advantage of the standard calibration curve recorded by using the UV–Vis spectrophotometer (at the absorption of 254 nm), the amount of un-bound proguanil drug was investigated from the supernatant. It was measured from the supernatant analysis that, about 72–80% of the used drug is getting adsorbed onto the EC-$MgHPO_4$ composite.

The studies of proguanil drug release kinetics from the surface of EC-$MgHPO_4$ composite was conducted as against two different parameters of pH, and temperature. Each time, a colloidal solution was prepared by taking 5 mg of EC-$MgHPO_4$-Proguanil into 2.5 mL of distilled water and the changes in the Proguanil drug concentration of the medium was recorded over a period. The actual Proguanil concentration that got released into the dispersion medium during the specified time intervals was quantified by making use of the standard calibration curve of Proguanil drug generated from the UV–Vis spectrophotometer [24]. From the analysis of results, the amount of Proguanil drug loading was calculated using the following formula.

Drug loading (mg/mg)
= Amount of drug in the composite/Amount of composite

2.4. Determination of physical parameters

2.4.1. Thickness

A digital micrometer with 0.1 μm of accuracy was used to measure the thickness of wet and dry tablets made from the composite.

2.4.2. Water uptake

In the application of electrochemistry, water uptake is a highly rated property. The water uptake values are estimated from the weight of dry and wet tablets which was immersed in water at 30 °C for a 24 h period [25].

2.4.3. Porosity

It is defined as the volume of water incorporated in the respective cavities per unit tablet volume from the data of water uptake.

$$Porosity = \left(\frac{W_w - W_d}{AL\rho_w}\right)$$

Where, A is the area of the tablet in mm^2, L the thickness of the tablet in mm and ρ_w the density of water in g/cm^3.

2.4.4. Bulk density (D_b)

It is defined as the ratio of total mass of powder to the bulk volume of powder. It was measured by inserting a specified weight of powder samples and passing it through a standard sieve of 85 μm into measuring cylinder and the difference in the initial and final weights are noted. The bulk density is determined from the formula given below which is expressed in *g/mL* [26],

$$D_b = \frac{M}{V_b}$$

Where M is the mass of powder and V_b is the bulk volume of the powder.

2.4.5. Tapped density (D_t)

It is defined as the ratio of total mass of the powder to the tapped volume of the powder. The volume was measured by tapping the powder for at least 750 times which was noted down continuously. The tapping was carried out regularly until the difference between successive volumes became <2%. It is expressed in *g/mL* which is given by relation as followed.

$$D_t = \frac{M}{V_t}$$

Where V_t is the tapped volume of the powder and M represents the mass of sample.

2.4.6. Angle of repose

The angle of repose (θ) was used to measure the frictional forces in a loose powder blend which indicated the flow properties of the powder. It is defined as maximum angle formed between the surface of the pile of powder and the horizontal plane.

$$\tan(\theta) = \frac{h}{r}$$
$$\theta = \tan^{-1}\left(\frac{h}{r}\right)$$

where h is the height and r is the radius, in which both are calculated in *cm*.

The blended powder was allowed to flow through the funnel fixed to a stand at definite height (h) through certain technique. The angle of repose denoted by θ was calculated by measuring the height and radius of the heap of powder formed. Special attention was paid and taken into account that the powder particles slip and slide on each other from the sides of the funnel.

2.4.7. Carr's compressibility index (%)

It has a natural ability which indicates powder flow properties and is expressed in the form percentage as given below.

$$I = \left[\frac{(D_t - D_b)}{D_t}\right] \times 100$$

Where D_t and D_b represents the tapped density and bulk density respectively.

2.4.8. Hausner ratio

Hausner ratio is an indirect index of ease of powder flow which is very specific. The magnitude of Hausner ratio is given by the formula mentioned below.

$$\text{Hausner ratio} = \frac{D_t}{D_b}$$

2.5. Instrumental analysis

The UV-1800 spectrophotometer (Shimadzu) was used to measure the UV–Vis spectra and the samples were prepared by taking water-methanol mixture as solvent; de-ionized methanol was used as reference as it gave a self sufficient clarity. An Alpha-FTIR spectroscopy (Bruker) was used for recording the Fourier transform-infrared (FT-IR) spectrum of the sample. For the measurements, an average of 200 scans was taken between 4000 and 600 cm^{-1} with a resolution of 4 cm^{-1} to give the final spectrum of the sample which was corrected at ambient temperature against the spectrum formed at the background. The particle's morphology and their size distribution in the EC-$MgHPO_4$ composite were performed using high resolution transmission electron microscopy (HRTEM) collected on a Tecnai G2 F20 instrument attached to EDAX (Energy dispersive analysis X-ray) analyzer. The field emission scanning electron microscopy (SEM) measurements were recorded on JEOL JSM-7600F instrument so as to understand the surface morphology of the composite. The powder X-ray diffraction (XRD) analysis was performed on an XRD 6000 instrument, Shimadzu by making use of nickel-filtered Cu Kα radiation.

2.6. Measurement of cell viability and proliferation

For the investigation of cell viability and proliferation induced by the EC-$MgHPO_4$ composite, the studies were performed following the treatment to two different cell lines of BRL-3A immortalized rat liver cells and H9c2 cardiomyoblast cells [27]. For the treatments, both the cells were grown independently in Dulbecco's modified eagle's medium (DMEM) supplemented with 10% Fetal bovine serum (FBS), 2 mM L-glutamine, 50 IU/mL penicillin, and 50 μg/mL streptomycin at 37 °C temperature maintained under 5% CO_2 in a humidified incubator. Following the harvesting of cells, both the cell types were counted individually (1×10^4 cells/well) and transferred to 96-well sterile microtiter plates in triplicates and incubated for another 24 h for proper adherence. When the cell growth reaches to 90% confluency, the testing material at different concentrations in the range of 25–500 μg/mL were treated to the cells individually and incubated for another 24 h. However, the cells incubated with 25 μL of phosphate buffered saline (PBS) and no EC-$MgHPO_4$ composite treatment was set as the control. Following the incubation time, the culture media was replaced with a solution containing 175 μL of fresh medium and 25 μL of MTT (3-[4,5-dimethylthiazol-2-yl]-2,5-diphenyltetrazolium bromide) reagent and then incubated for another 4 h at 37 °C under 5% CO_2. At the completion of incubation period, the medium was replaced with a 100 μL of dimethyl sulfoxide to solubilize the formazan crystals formed as part of the cell's reaction with MTT reagent. The optical density was taken at an excitation wavelength of 575 nm using μQuant™ enzyme-linked immunosorbent assay plate reader (BioTek Instruments) and the results expressed are the percentage proliferation with respect to vehicle-treated cells. The values shown are the mean ± SD of three individual experiments.

3. Results and discussion

3.1. Physical characterization

The physico-chemical parameters such as water uptake, thickness, porosity etc. significantly influences the acceptability of the produced tablets of EC-$MgHPO_4$ composite and for that reason, the powdered flow characteristics are calculated and are shown in Table 1. From the table, the water uptake is expressed in the form of volume fraction of water in the material phase [28]. The water accommodated in the void space generally because of the water absorption which occurred due to the presence of hydrophilic functional groups and hydrogen bonding [29].

Also from the table, the value of Carr's index (compressibility index) lies in the range of 11.11% and for any material which has the Carr's index in the range of 5–12 meaning that the material has extraordinary ability to flow; however, if the range is above 12 meaning that the material has poor performance to flow. Similarly, the value of Hausner's ratio observed to be 1.125 which also resembles that it has good property to flow and above 1.25, the material loses the property to flow. In general, a material of Hausner's ratio <1.2 is an indicative of a free-flowing powder with low inter particulate friction [30].

The comparison of the surface morphology and particle size distribution for the $MgHPO_4$ and EC-$MgHPO_4$ composite obtained from the HRTEM and SEM analysis are shown in Fig. 2(a-d). From the comparison of images between Fig. 2a and b, one can see clearly for the presence of EC material, in addition to an observation that the $MgHPO_4$ particles are irregularly shaped. Also, Fig. 2c provides the visual proof for the presence of EC coverage onto the $MgHPO_4$ core, in addition to the porous nature of the EC polymer which promotes for the adsorption/encapsulation of drug. Further from Fig. 2d, the mean crystalline size of $MgHPO_4$ particles (as marked in Fig. 2b) in the EC-$MgHPO_4$ composite were measured to be around 52 nm. Thus from the analysis of microscopic images, it can be confirmed primarily for the presence of EC matrix and also the persistence of $MgHPO_4$ crystals in the final composite of EC-$MgHPO_4$.

Further, the powdered XRD and the EDAX analysis for the EC-$MgHPO_4$ composite are shown in Fig. 3(i-ii). From the EDAX analysis shown in Fig. 3(ii), the appearance of atomic peaks for C, O, Mg and P confirms the presence of corresponding elements in the final composite of EC-$MgHPO_4$ [31]. Also, the appearance of highly resolved intense peaks at 2θ Bragg angle indicates the crystallinity of the EC-$MgHPO_4$ composite. From the diffraction pattern shown in Fig. 3(i), the broad peak for the EC matrix at 2θ of around 20° and the sharp-intense peak around 15° getting changed and observed to be around 18° following the composite formation. These changes are attributed to the occurrences of the changes in the bond length and structure as a result of doping. However, the XRD peaks observed for the $MgHPO_4$ crystal were assigned the [hkl] planes of [111], [002], [202], [213], [014], [141], [412], [125], [250], [600], and [603], there by confirming for the presence of $MgHPO_4$ to be in orthorhombic crystal form in the final composite of EC-$MgHPO_4$ [32].

Fig. 4 shows the UV–Vis absorption spectral comparison for the samples of pure EC and Proguanil drug with that of Proguanil-loaded EC-$MgHPO_4$ composite. From the figure, the absorption maximum for the pure Proguanil drug is observed to be around 254 nm wavelength and is attributed for the π-π* transitions in small electronically conjugated domains generally at aromatic C—C ring. However, following its loading onto EC-$MgHPO_4$ composite, the peak becoming broader and is

Table 1
Physicochemical parameters of the EC-$MgHPO_4$ tablets.

Parameters	Results
Water uptake	8.2 ± 0.054%
Thickness	2.8 mm
Porosity	0.46
Bulk density	0.320 g/mL
Tapped density	0.360 g/mL
Carr's index	11.11%
Hausner's ratio	1.125
Angle of response	33.04°

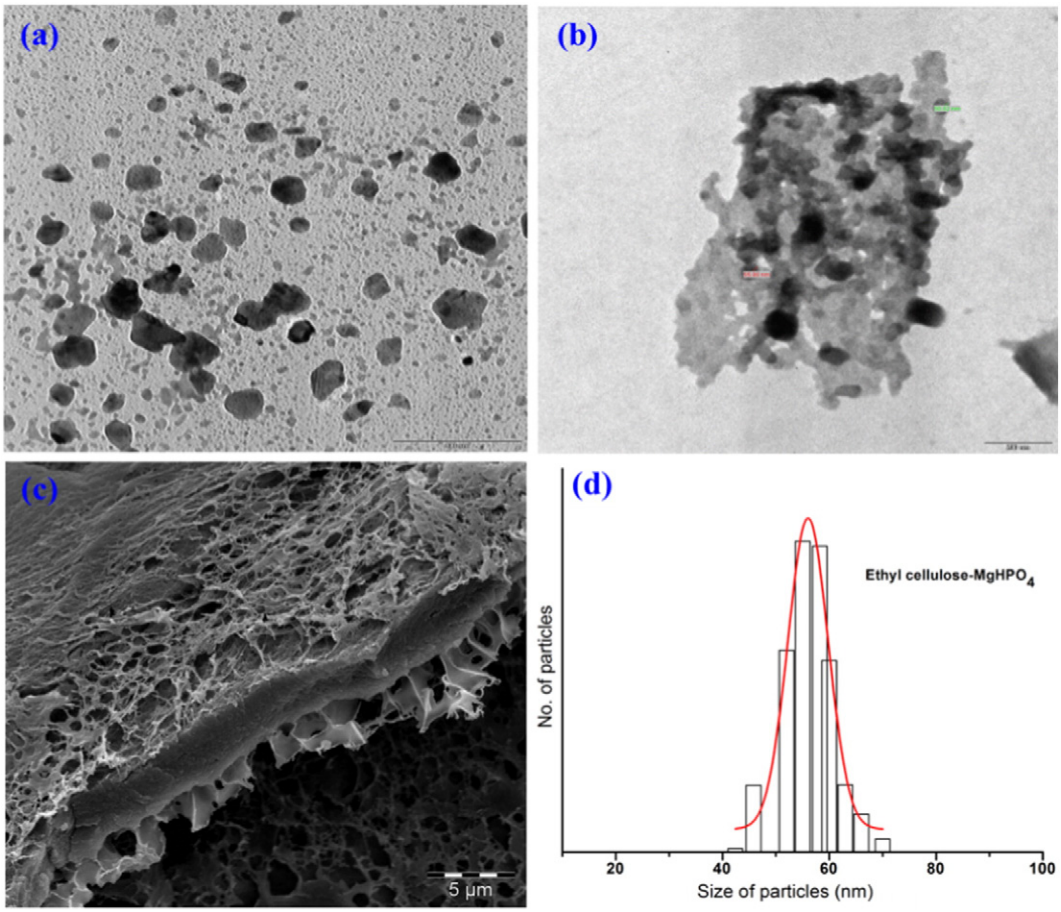

Fig. 2. HRTEM images of $MgHPO_4$ (a), and EC-$MgHPO_4$composite (b). The surface morphology of EC-$MgHPO_4$ composite obtained from SEM is shown in (c) and the particles size distribution of the final composite in (d).

observed to be around an absorption maximum of 258 nm, thereby primarily providing for the confirmation for the effective loading [33].

A step-by-step analysis by means of FT-IR spectroscopy for the organic-inorganic hybrids of EC-$MgHPO_4$ composite before and after its loading with Proguanil drug is shown in Fig. 5(a-b). From the Fig. 5a, the stretching and bending vibrations of C—H groups from the EC bonding in the composite of EC-$MgHPO_4$ are observed to be around 1650 and 1240 cm^{-1} respectively [34]. The C-O-C stretching in the cyclic ether of EC was in corresponding to the strong peak at 1010 cm^{-1} and the hydrogen bonded OH stretching vibration was noted by the intense band

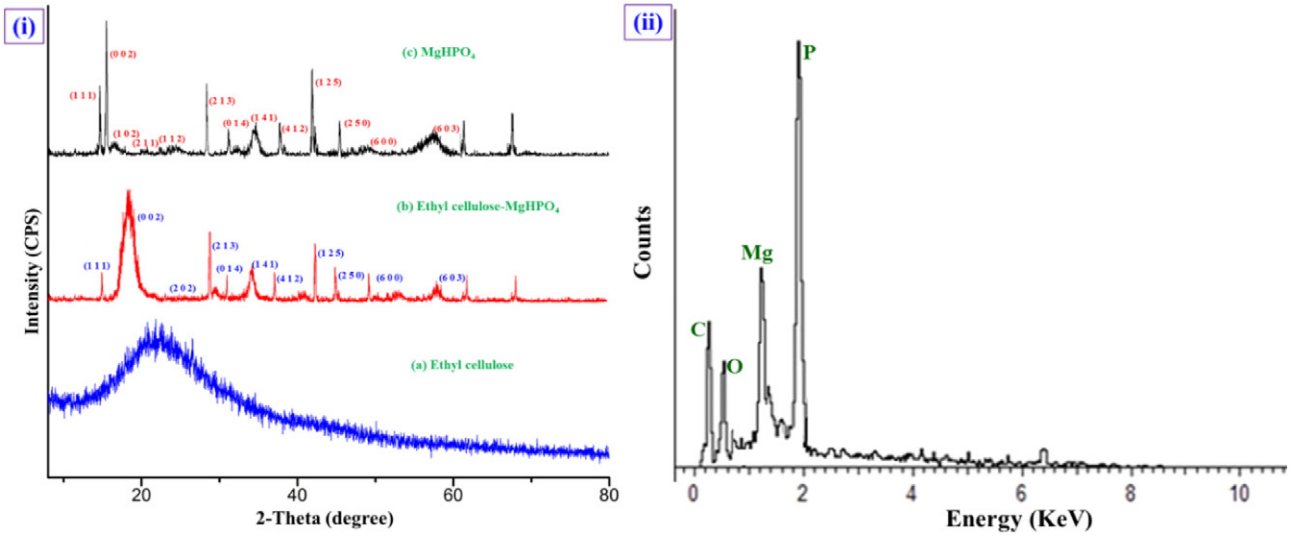

Fig. 3. (i) Comparison of the XRD spectrums of EC, $MgHPO_4$, and EC-$MgHPO_4$ composite; (ii) EDAX of EC-$MgHPO_4$ composite.

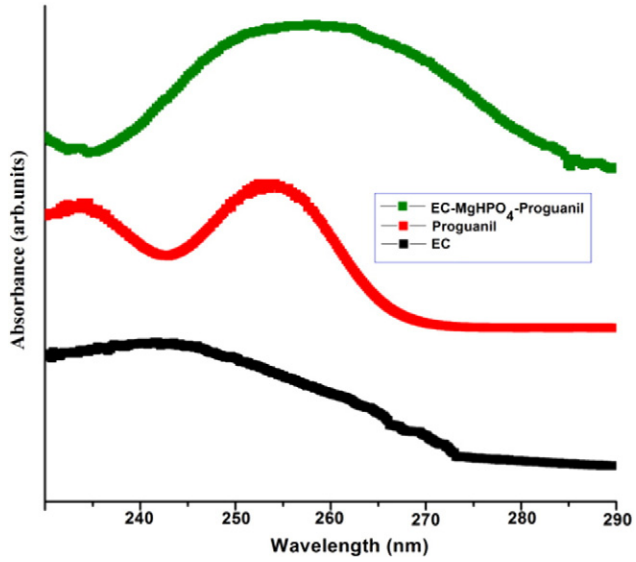

Fig. 4. Comparison of the UV–Vis spectra of EC, Proguanil, and EC-$MgHPO_4$-Proguanil composite.

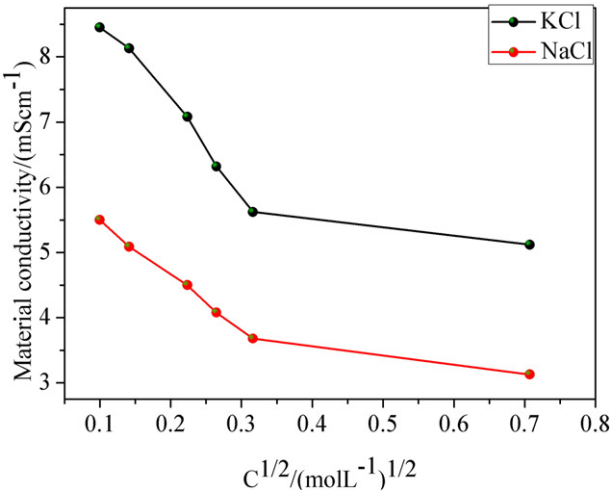

Fig. 6. Plot of material conductivity vs. concentration for the EC-$MgHPO_4$ composite when tested under a 1:1 electrolyte concentration at 25 ± 0.1 °C.

near 3487 cm^{-1}; the bands near 882 and 641 cm^{-1} are attributed to the vibrations of PO_4^{3-} [35–36]. The superposition of Mg metal–oxygen stretching vibration was apprehensive due to the sharp peaks in the region of 495 cm^{-1}. A less broad peak in the region of 1018 cm^{-1} was generally due to the presence of HPO_4^{2-} [36]. Similarly, for the Fig. 5b, the observation of a broad peak around 3500 cm^{-1} may be due to the mixed peaks from the stretching vibrations of N—H of Proguanil, O—H of EC, and =C-H of both. The other bonds in the Proguanil drug such as, the stretching vibrations of C=N bond around 1745 cm^{-1}, C=C at 1640 cm^{-1}, C—N at 1060 cm^{-1}, C—Cl at 692 cm^{-1}, and C—N bending at 1480 cm^{-1}, in the final composite of EC-$MgHPO_4$-Proguanil [37]. The comparative analysis of spectrums of UV–Vis and FT-IR therefore confirms for the successful loading of Proguanil drug onto the EC-$MgHPO_4$ composite.

3.2. Studies of conductivity

Fig. 6 shows the variations in the conductivity for EC-$MgHPO_4$ composite in the presence of 1:1 electrolyte concentration when recorded at room temperature. Since the solution conductivity is a dependent of dilution, it can be noted from the figure that the electrical conductivity seems to be increased rapidly with dilution. The other two factors on which the solution conductivity depends are the number of ions present in the solution and the speed of ions. The increase of conductivity with increase in dilution was basically due to an increase in the degree of dissociation of the electrolytes and decreased force of attraction between the ions. With the enhancement of dilution, the influence of one ion on the movement of other ion tends to be decreased. One ion becomes completely independent of the other ion at the specific dilution. At the specific point, it renders to contribute maximum towards the conductivity of solution [38]. The conductivity is noticed to be increased with a decrease in the concentration of electrolytes in both the cases as shown in the Fig. 6 [39]. When the concentration is more, the forces of attraction between the ions increases and the movement of ions in the solution gets decreased. Hence, it is an obligatory observation that the conductivity decreases with concentration. In accordance with a size of the hydrated radii of the ions, the conductivity of EC-$MgHPO_4$ material for 1:1 electrolyte solution was found to be decreased in the order $K^+ > Na^+$. The higher absorption is resulted by the invasion of ions of smaller hydrated radii into the pores of material.

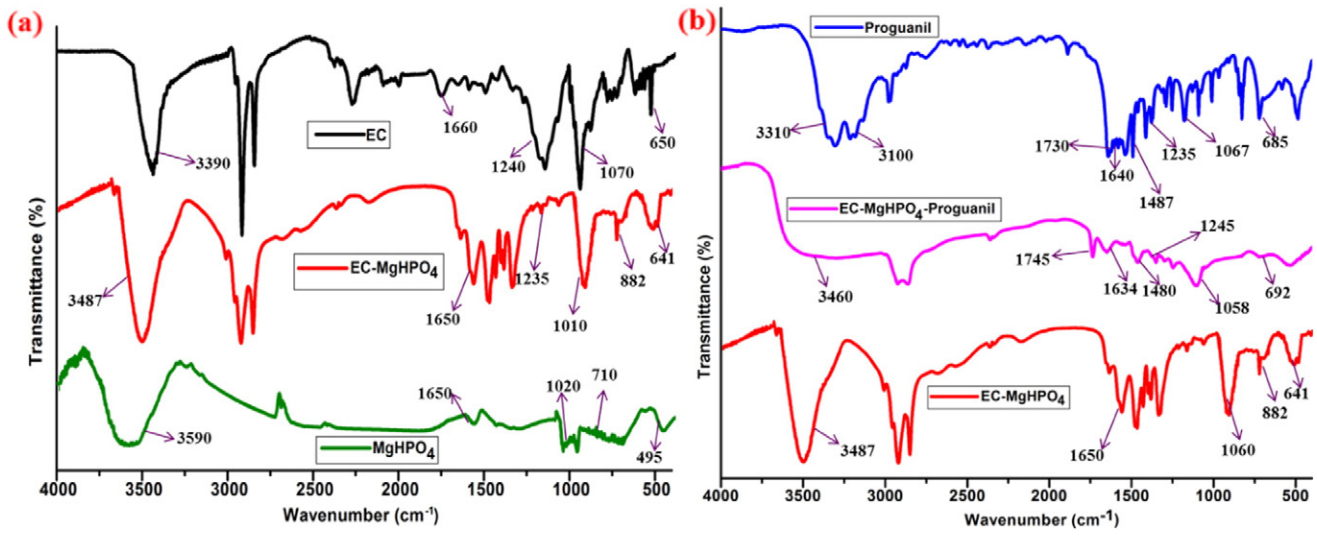

Fig. 5. FT-IR analysis of the formation of EC-$MgHPO_4$ composite from EC and $MgHPO_4$ (a), and the formation of EC-$MgHPO_4$-Proguanil from Proguanil and EC-$MgHPO_4$ (b).

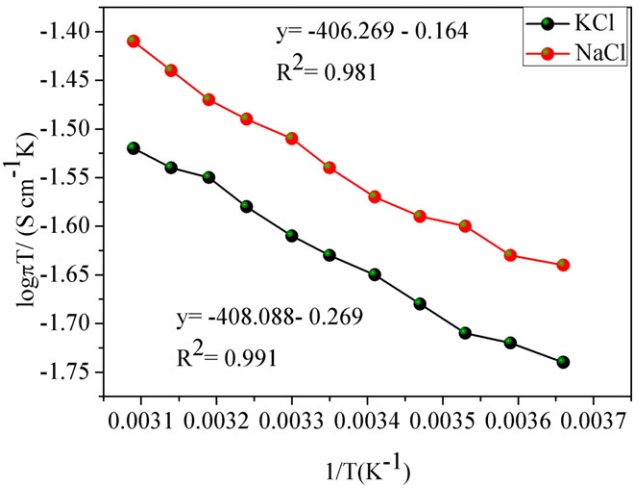

Fig. 7. Plot of material conductivity vs. temperature for the EC-$MgHPO_4$ composite when tested under a 0.5 M of 1:1 electrolyte solution at (25–50) ± 0.1 °C.

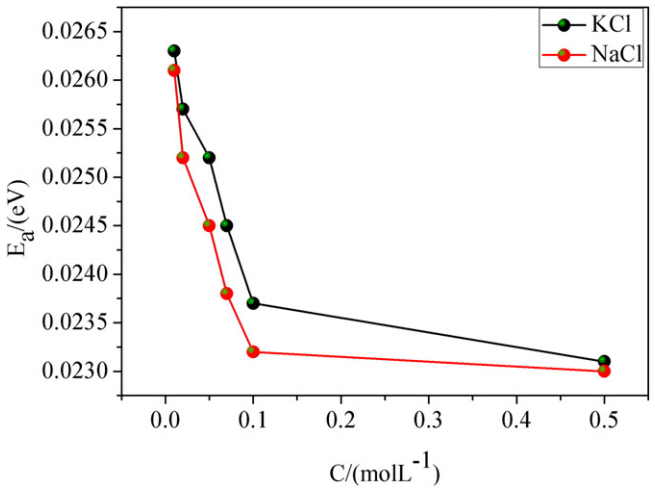

Fig. 8. Plot of activation energy vs. concentration for the EC-$MgHPO_4$ composite under 1:1 electrolyte concentration at 25 ± 0.1 °C temperature.

The Arrhenius expression gives the relation for the dependence of conductivity on temperature [40]:

$$\sigma T = \sigma_0 \exp\left(\frac{E_a}{\kappa T}\right)$$

Where, σ_0 is the pre-exponential factor, T the temperature, κ the constant and E_a the activation energy of ionic motion.

For obtaining the activation energy, the conductivity data was applied to the above given equation. Fig. 7 shows the temperature dependence of conductivity for the EC-$MgHPO_4$ composite according to the Arrhenius equation and the same conductivity behavior was manifested by the other sample as well. For the KCl and NaCl solutions, the increase of temperature causes an increase in the movement of ions which finally gave an outcome of increased conductivity. It was also quite apparent to observe that the conductivity for 1:1 electrolyte was highly dependent on temperature.

The value of activation is estimated by plotting the graph between log πT and $1/T$ in Fig. 7. The graph shows a straight line where the slope is equal to $-E_a/2.303R$ or $-E_a/5.476$, from which the value of E_a can be determined. Table 2 shows the values of activation energies for the 1:1 electrolytes of KCl and NaCl solutions. The super-ionic nature of the material in the temperature region is responsible for sustaining the low values of activation energy. Similarly, the variation in the activation energies for the EC-$MgHPO_4$ composite when tested at 1:1 electrolyte solutions of KCl and NaCl is shown in Fig. 8. From the figure, the activation energy seems to be less for NaCl as compared against the KCl solution and this decrease is in accordance with the degree of hydration and the nature of the solvent, where the size and charge of the ion has a significant influence towards the activation energy.

By maintaining the concentration of the relevant ion constant (1×10^{-2} mol L^{-1}), the potentials of the EC-$MgHPO_4$ composite were calculated at a pH range of 1–12 for the KCl solution as shown in Fig. 9. The pH was adjusted by putting a drop of 0.1 M HNO_3 or NaOH solution, and at each pH value the potential of EC-$MgHPO_4$ was determined. The Fig. 9 indicates that the potential remains constant in the range of 5.0–7.5 and this pH is regarded as best for the composite due to its stable performance. Further, the potential starts decreasing rapidly above pH 8 because of the formation of hydroxide ions. The material sensor responds to hydrogen ions at lower pH where the potential increases [21].

Table 2
Activation energies of conduction for the EC-$MgHPO_4$ composite when tested under 0.5 M of 1:1 electrolytes at (25–50) ± 0.1 °C.

Electrolyte (mol L^{-1})	Activation energy (eV)
KCl	0.0231
NaCl	0.0230

3.3. Studies of drug release and cytotoxicity

The release profiles of drug, Proguanil from the EC-$MgHPO_4$ composite as a function of pH and temperature is shown in the Fig. 10(a-b). From the Fig. 10(a) which shows the comparison of the drug release profiles as against the changes in pH indicates that the highest release seems to be observed for the neutral pH of 7.4, followed by acidic and basic pHs. When the pH of the medium was maintained at neutral, we observed the highest release of 87% Proguanil drug that got loaded after 90 mins of incubation. However, for the acidic and basic pHs, the highest percentages of Proguanil that got released into the medium were observed to be 74% and 70% (respectively) before the release profile reaches to an equilibrium. The variations in the observed release profiles of Proguanil drug from the same EC-$MgHPO_4$ composite in accordance to the solution pH can be attributed to the physico-chemical characteristics of the EC matrix. For example, at the basic pH, the total reduction of drug release from the EC matrix as compared to others can be ascribed to its insolubility which is obtained by means of deprotonation. However, the acidic pH promotes for the enhanced crosslinking within the EC molecules thereby decreasing the rate of

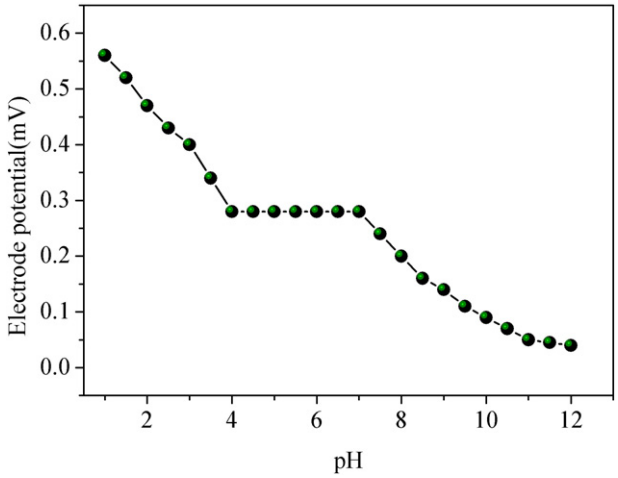

Fig. 9. Effect of pH for the KCl solutions (1×10^{-2} mol L^{-1}) on the potential response of EC-$MgHPO_4$ composite.

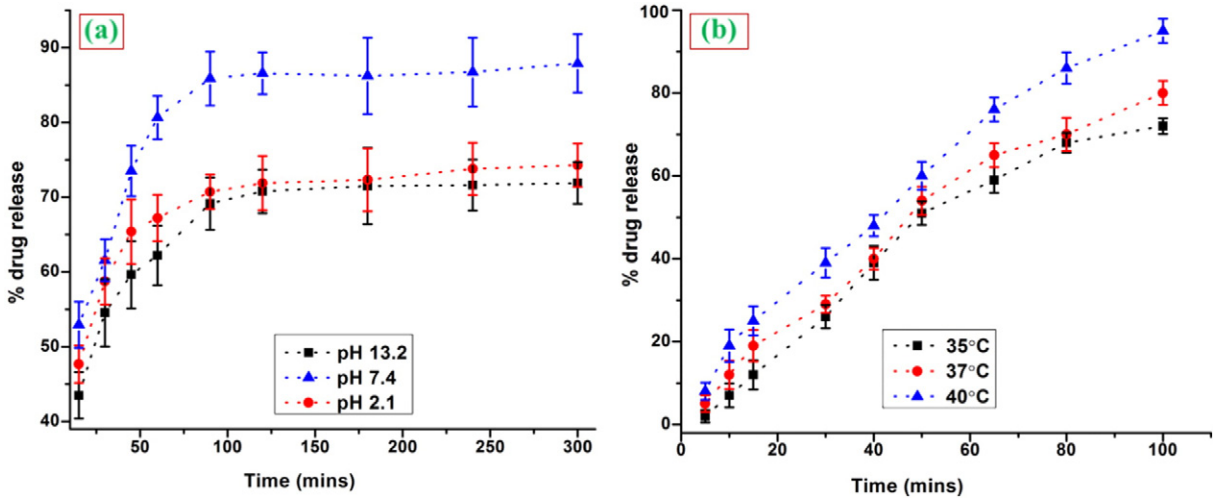

Fig. 10. Proguanil drug release profiles of EC-$MgHPO_4$ when treated against (a) different pH of 2.1, 7.4 and 13.2 at 37 °C temperature and (b) different temperatures of 35 °C, 37 °C, and 40 °C at a pH of 7.4.

drug release into the medium. Because of the absence of deprotonation or crosslinking at the neutral pH, the Proguanil release is unaffected by the physiological changes [41–42]. Further, from Fig. 10(b), we observed an increase in the release rate of drug in accordance with the temperature, i.e. 40 °C > 37 °C > 35 °C. This increased release profile with respect to the temperature of releasing medium can be ascribed to an increase in the activation energy provided by the dispersion medium. This temperature dependent release mechanism from the surface of EC matrix can further be explored to control the drug release profiles externally by means of increasing the local body temperature for in vivo purposes. Thus, the results of the drug release studies therefore provides a proof for the applicability of our synthesized EC-$MgHPO_4$ composite for controlled and sustained release applications in the pharmaceutical and healthcare sector.

The comparison of the cell viability and proliferation studies following the treatment of $MgHPO_4$ and EC-$MgHPO_4$ composite to the two different cell lines of BRL-3A liver cells and cardiomyoblasts are shown in Fig. 11(a-b). From the analysis of results, one can see clearly that both the tested compounds do not induce any significant levels of toxicity to both the cell cultures. The maximum reduction in the viability of cells observed for $MgHPO_4$ and EC-$MgHPO_4$ composite at the highest concentration of 500 μg/mL are 85% and 78% for BRL-3A cells, while for H9c2 it is 91% and 79% respectively. These results are anticipated because of the presence of EC biopolymer which is considered to be a safe biomaterial due to its six membered hexagonal structure and stable bonding. Also, the absence of oxidative elements or groups both in the $MgHPO_4$ and EC contributed for its non-toxic behavior, thereby providing an experimental evidence for the applicability of the prepared EC-$MgHPO_4$ composite for drug delivery, biosensor and scaffolding applications.

4. Conclusion

In conclusion, we report the synthesis and characterization of EC-$MgHPO_4$ composite that can be useful for different application sites of biosensor, drug delivery, scaffolding and qualitative analysis. From the physical characterization of the composite, the HRTEM and EDAX confirmed for the composite formation and the particles size investigated to fall around 52 nm. The powdered XRD studies confirmed for the persistence of $MgHPO_4$ crystals even after the composite formation, while the UV–Vis and FT-IR analysis provided information related to the bonding of $MgHPO_4$ with that of EC groups by physical means. Also, the conductivity of EC-$MgHPO_4$ estimated by making use of uni-univalent electrolyte solutions of KCl and NaCl proved that the material is electrically conductive and the conductivity follows the order of KCl > NaCl. The composite exhibited efficient conductivity in the pH range of 5.0 to 7.5 because of the stable bonding and the specific properties of the material were found to carry good conductivity due to its narrow surface opening and porous nature. Similar to the electrical conductivity, the Proguanil drug kinetic studies also investigated to show highly efficient drug loading of about 82% onto the EC matrix and some enhanced release profiles at the neutral pH as compared against acidic and basic

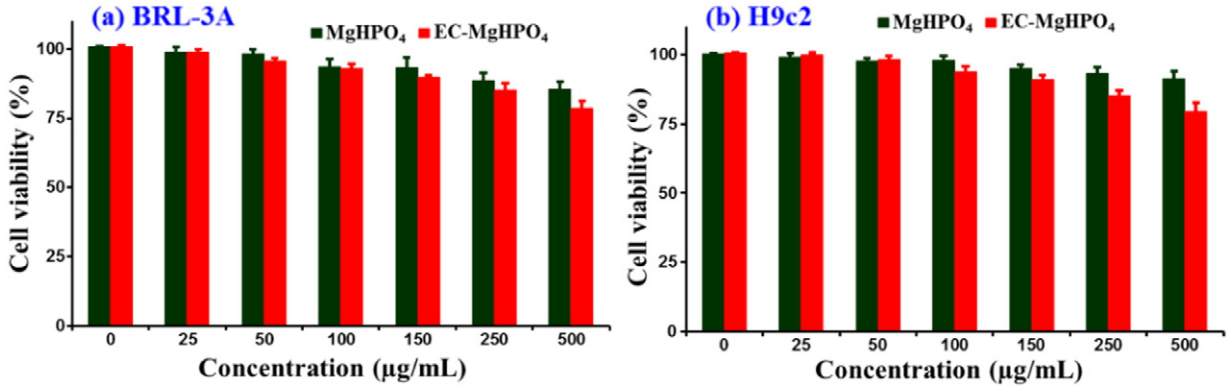

Fig. 11. Comparison of the cell viability and proliferation studies of $MgHPO_4$ and EC-$MgHPO_4$ composite when tested against (a) BRL-3A liver cells and (b) H9c2 cardiomyoblast cells (concentration range 0–500 μg/mL, 24 h).

pH. If we ignore the variations in the release profiles (which is not actually much) due to slight changes in the applied parameters, we observed significant increase in the release of loaded Proguanil drug (87%) from the matrix over a 90 min period. This property of effective drug encapsulation onto the EC matrix can particularly be helpful for the delivery of light or temperature sensitive drugs so as to stabilize the formulation for longer periods, in addition to developing combinational drug delivery systems to cure multiple symptoms. However, the controlled release properties can best be suitable for the delivery of powerful *anti*-cancer drugs where they are prone to maintain unwanted side effects and high toxicities towards non-target tissues. In addition, the results of cell viability and proliferation provided a proof for the non-toxic nature of the EC-$MgHPO_4$ composite and thereby supporting its role in the development of sustained drug delivery systems and biosensor related applications. In general, employing the organic-inorganic components organized in complex structures for the current biomedical sector can be highly beneficial due to some enhanced properties associated with this combination such as mechanical (toughness and Young's modulus), collagen fiber networking, conductivity, functional group orientation, stability, biocompatibility, and decreased toxicity, to mention some. Further studies are under progress to adsorb the antibody bound graphene oxide material with our EC-$MgHPO_4$ composite in order to investigate the efficacy of detecting malaria diseased cells by means of electrochemical measurements.

Conflict of interest

The authors declare no conflict of interest with this work.

Acknowledgements

This project was financially supported by King Saud University, vice deanship of research chairs.

References

[1] A. Arakaki, K. Shimizu, M. Oda, T. Sakamoto, T. Nishimura, T. Kato, Biomineralization-inspired synthesis of functional organic/inorganic hybrid materials: organic molecular control of self-organization of hybrids, Org. Biomol. Chem. 13 (2015) 974–989.
[2] D.B. Hazer, M. Sakar, Y. Dere, G. Altinkanat, I.M. Ziyal, B. Hazer, Antimicrobial effect of polymer-based silver nanoparticle coated pedicle screws: experimental research on biofilm inhibition in rabbits, Spine 41 (2016) E323–E329.
[3] B. Hazer, E. Akyol, Efficiency of gold nano particles on the autoxidized soybean oil polymer: fractionation and structural analysis, J. Am. Oil Chem. Soc. 93 (2016) 201–213.
[4] S. Korkut, S. Uzuncar, M.S. Kilic, B. Hazer, Electrochemical, continuous-flow determination of p-benzoquinone on a gold nanoparticles poly(propylene-co-imidazole) modified gold electrode, Instrum. Sci. Technol. 44 (2016) 614–628.
[5] E. Berber, N. Horzum, B. Hazer, M.M. Demir, Solution electrospinning of polypropylene-based fibers and their application in catalysis, Fibers Polym. 17 (2016) 760–768.
[6] T. Arfin, N. Yadav, Impedance characteristics and electrical double-layer capacitance of composite polystyrene-cobalt-arsenate membrane, J. Ind. Eng. Chem. 19 (2013) 256–262.
[7] R.A.S. Ferreira, P.S. André, L.D. Carlos, Organic–inorganic hybrid materials towards passive and active architectures for the next generation of optical networks, Opt. Mater. 32 (2010) 1397–1409.
[8] T. Nishimura, Macromolecular templates for the development of organic/inorganic hybrid materials, Polym. J. 47 (2015) 235–243.
[9] J. Zhu, X.T. Dong, X.L. Wang, Y.Z. Wang, Preparation and properties of a novel biodegradable ethyl cellulose grafting copolymer with poly(p-dioxanone) side-chains, Carbohydr. Polym. 80 (2010) 350–359.
[10] E.A. Abdel-Razik, Photoinduced graft copolymerization of ethyl acrylate, methyl methacrylate and methyl acrylate onto ethyl cellulose in homogeneous media, J. Photochem. Photobiol., A 107 (1997) 271–274.
[11] N.H. Parikh, S.C. Porter, B.D. Rohera, Aqueous ethyl cellulose dispersion of ethyl cellulose. I. Evaluation of coating process variables, Pharm. Res. 10 (1993) 525–534.
[12] W.J. Lin, T.L. Wu, Modification of the initial release of a highly water-soluble drug from ethyl cellulose microspheres, J. Microencapsul. 16 (1999) 1639–1646.
[13] M.E. Hezzat, M. Et-tabirou, L. Montagne, E. Bekaert, G. Palavit, A. Mazzah, T. Dhamelincourt, Structure and AC conductivity of sodium-lead-cadmium metaphosphate glasses, Mater. Lett. 58 (2003) 60–66.
[14] P.F. James, Glass ceramics: new compositions and uses, J. Non-Cryst. Solids 181 (1995) 1–15.
[15] M.J.J. Weber, Science and technology of laser glass, J. Non-Cryst. Solids 123 (1990) 208–222.
[16] B.C. Sales, L.A. Boatner, Lead-iron phosphate glass: a stable storage medium for high-level nuclear waste, Science 226 (1984) 45–48.
[17] V. Koleva, V. Stefov, Phosphate ion vibrations in dihydrogen phosphate salts of the typeM(H2PO4)·2H2O (M = Mg, Mn, Co, Ni, Zn, Cd): spectra-structure correlations, Vib. Spectrosc. 64 (2013) 89–100.
[18] A.S. Wagh, Recent progress in chemically bonded phosphate ceramics, ISRN Ceram. 2013 (2013) 983731 (20 pp.).
[19] P. Kubáň, P.C. Hauser, A review of the recent achievements in capacitively coupled contactless conductivity detection, Anal. Chim. Acta 607 (2008) 15–29.
[20] P. Kubáň, P.C. Hauser, Ten years of axial capacitively coupled contactless conductivity detection for CZE-a review, Electrophoresis 30 (2009) 176–188.
[21] T. Arfin, C. Kumar, Synthesis, characterization, conductivity and antibacterial activity of ethyl cellulose manganese(II) hydrogen phosphate, Anal. Bioanal. Electrochem. 6 (2014) 403–421.
[22] T. Arfin, Rafiuddin, Thermodynamics of ion conductivity of alkali halides across a polystyrene-based titanium arsenate membrane, Electrochim. Acta 55 (2010) 8628–8631.
[23] T. Arfin, R. Bushra, R.J. Kriek, Ionic conductivity of alkali halides across a polyaniline zirconium(IV)-arsenate membrane, Anal. Bioanal. Electrochem. 5 (2013) 206–221.
[24] F. Mohammad, N.A. Yusof, Doxorubicin-loaded magnetic gold nanoshells for a combination therapy of hyperthermia and drug delivery, J. Colloid Interface Sci. 434 (2014) 89–97.
[25] T. Arfin, A. Falch, R.J. Kriek, Evaluation of charge density and the theory for calculating membrane potential for a nano-composite nylon-6,6 nickel phosphate membrane, Phys. Chem. Chem. Phys. 14 (2012) 16760–16769.
[26] S. Mohanty, R. Mohapatra, S. Patra, D.K. Sahoo, Formulation and in-vitro evaluation of azithromycin mouth dissolving tablets using super disintegrants, Res. J. Pharm., Biol. Chem. Sci. 4 (2013) 452–461.
[27] F. Mohammad, T. Arfin, Cytotoxic effects of polystyrene–titanium–arsenate composite in cultured H9c2 cardiomyoblasts, Bull. Environ. Contam. Toxicol. 91 (2013) 689–696.
[28] R.P. Pandey, V.K. Shahi, Aliphatic-aromatic sulphonated polyimide and acid functionalized polysilsesquioxane composite membranes for fuel cell applications, J. Mater. Chem. A 1 (2013) 14375–14383.
[29] M. Kumar, S. Singh, V.K. Shahi, Cross-linked poly(vinyl alcohol)-poly(acrylonitrile-co-2-dimethylamino ethyl methacrylate) based anion-exchange membranes in aqueous media, J. Phys. Chem. B 114 (2010) 198–206.
[30] R.B. Shah, M.A. Tawakkul, M.A. Khan, Comparative evaluation of flow for pharmaceutical powders and granules, AAPS PharmSciTech 9 (2008) 250–258.
[31] A. Farzadi, F. Bakhshi, M.S. Hashjin, M.A. Eydivand, N.A. Osman, Magnesium incorporated hydroxyapatite: synthesis and structural properties characterization, Ceram. Int. 40 (2014) 6021–6029.
[32] K.K. Bamzai, R. Gupta, S. Suri, V. Singh, Dielectric behavior of mixed cadmium magnesium hydrogen phosphate crystal, Adv. Mater. Lett. 5 (2014) 89–95.
[33] N.S. Jadhav, K.G. Lalitha, Spectroscopic method development and validation for simultaneous estimation of atovaquone and aproguanil in tablet dosage form, World J. Pharm. Pharm. Sci. 3 (2014) 1986–1994.
[34] D.M. Patel, R.H. Jani, C.N. Patel, Design and evaluation of colon targeted modified pulsincap delivery of 5-fluorouracil according to circadian rhythm, Int. J. Pharm. Investig 1 (2011) 172–181.
[35] Y. Bai, C. Jiang, Q. Wang, T. Wang, A novel high mechanical strength shape memory polymer based on ethyl cellulose and polycaprolactone, Carbohydr. Polym. 96 (2013) 522–527.
[36] H. Assaaoudi, Z. Fang, I.S. Butler, D.H. Ryan, J.A. Kozinski, Characterization of a new magnesium hydrogen orthophosphate salt, Mg3·5H2(PO4)3, synthesized in supercritical water, Solid State Sci. 9 (2007) 385–393.
[37] N.R. Pai, S.S. Sawant, Synthesis of impurities of proguanil hydrochloride, an antimalarial drug, Der Pharm. Chem. 6 (2014) 176–187.
[38] T. Arfin, S. Fatima, Conductometric studies with polystyrene calcium phosphate membrane, Asian J. Adv. Basic Sci. 2 (2013) 1–14.
[39] M.N. Beg, K. Ahmad, I. Altaf, M. Arshad, Ionic transport of alkali chlorides in parchment supported cupric orthophosphate membrane and application of absolute reaction rate theory, J. Membr. Sci. 9 (1981) 303–311.
[40] T. Arfin, F. Mohammad, DC electrical conductivity of nano-composite polystyrene-titanium-arsenate membrane, J. Ind. Eng. Chem. 19 (2013) 2046–2051.
[41] M.A. Quadir, E. Chanda, S.S. Haider, M.D. Reza, B.K. Datta, Evaluation of ethylcellulose as matrices for controlled release drug delivery, Pak. J. Pharm. Sci. 18 (2005) 29–34.
[42] L. Mu, S.S. Feng, Fabrication, characterization and in vitro release of paclitaxel (Taxol®) loaded poly (lactic-co-glycolic acid) microspheres prepared by spray drying technique with lipid/cholesterol emulsifiers, J. Control. Release 76 (2001) 239–254.